Received: 19 October 2023 | Revised: 22 February 2024 | Accepted: 2 March 2024
DOI: 10.1002/aic.18439

AIChE JOURNAL

RESEARCH ARTICLE

Separations: Materials, Devices and Processes

Highly efficient capture of CO_2 through the synergy of intramolecular amines within piperazine-derived alcoholamines

Shaojun Jia[1] | Yao Jiang[1] | Songtao Zheng[1] | Yi Li[1] | Yan Wu[1] | Xiao-Qin Liu[2] | Peng Cui[1]

[1]School of Chemistry and Chemical Engineering, Hefei University of Technology, Hefei, China

[2]State Key Laboratory of Materials-Oriented Chemical Engineering, College of Chemical Engineering, Nanjing Tech University, Nanjing, China

Correspondence
Yao Jiang and Peng Cui, School of Chemistry and Chemical Engineering, Hefei University of Technology, Hefei, 230009, China.
Email: yjiang@hfut.edu.cn and cuipeng@hfut.edu.cn

Funding information
Fundamental Research Funds for the Central Universities, Grant/Award Number: JZ2023HGTB0226; Graduate Academic Innovation Project of Anhui Province, Grant/Award Number: 2022xscx019; Major Science and Technology Project of Anhui Province, Grant/Award Number: 201903a07020004; State Key Laboratory of Materials-Oriented Chemical Engineering, Grant/Award Number: SKL-MCE-22B11; National Natural Science Foundation of China, Grant/Award Number: 22208078

Abstract

Amine-scrubbing-based chemical absorption remains a prominent CO_2 capture process. However, the overall efficiency of conventional amine absorbents is hard to meet the ever-increasing demands for CO_2 capture. Consequently, developing powerful absorbents for efficient and cost-effective CO_2 capture is greatly important but challenging. Here, a new type of amine absorbent with improved solubility and stability was achieved by substituting the secondary amino groups in piperazine (PZ) with aminoethyl and hydroxyalkyl moieties. The developed amine absorbent presents superior CO_2 absorption/desorption abilities through the synergy of their intramolecular amines, leading to a low regeneration energy consumption of 2.56 $GJ{\cdot}t^{-1}$ CO_2. Moreover, the enhancement of CO_2 capture and the corresponding mechanism were elucidated using density functional theory calculations and nuclear magnetic resonance analysis. Such newly developed amine absorbent with excellent CO_2 capture performance are expected to greatly contribute to ongoing efforts toward carbon neutrality.

KEYWORDS
absorption mechanism, amine absorbent, carbon neutrality, chemical absorption, CO_2 capture

1 | INTRODUCTION

Increasing carbon dioxide (CO_2) emissions intensify global warming and climate change and seriously affect human activities and life.[1–3] At present, heavy industries that combust fossil fuels, including power plants and chemical industries, are the primary sources of CO_2, accounting for more than 60% of the total emissions from process industry.[4–6] Reducing CO_2 emissions has become a severe challenge for human society. Carbon capture, utilization, and storage (CCUS) technology is considered to provide an efficient route to achieve carbon neutrality.[7] Among various CCUS technologies, amine-scrubbing-based chemical absorption has always been the most practical technology as it offers advantages over other CCUS processes, such as distillation,[8] membrane separation,[9] and adsorption[10] in terms of rapid separation rate, high capture capacity, and long-term reusability,[11–14] making it more economical and efficient. The absorbent is the key to chemical absorption. The variety and structure of the absorbent not only affect the kinetics and thermodynamics of CO_2 absorption/desorption but are also impact the equipment and operating costs of the technological process.[15] Therefore, the development of powerful absorbents into chemical absorption is of paramount importance for efficient and cost-effective CO_2 capture.

Typical monoamine-based absorbents, such as monoethanolamine (MEA),[16] diethanolamine (DEA),[17] and *N*-methyldiethanolamine (MDEA)[18] have contributed significantly to the chemical absorption of CO_2 over an extended period. However, their overall efficiencies are unable to meet ever-increasing CO_2 capture demands because monoamine molecules only contains a single amine group.[19] In addition,

   AIChE J. 2024;70:e18439.
https://doi.org/10.1002/aic.18439

while chain polyamines presented superior CO_2 capture than that of the monoamines and the blended amines due to the interplay of various intramolecular amine groups,[20,21] their reusability is severely restricted due to problems associated with easy degradation and volatilization. Ring-structured molecules are known for their relatively robust physicochemical stabilities,[22,23] as evidenced by the negligible degradation of piperazine (PZ) during the chemical absorption of acid gases.[24] Moreover, the low steric hindrance of PZ can help to enhance the absorption rate for acid gases.[25,26] Unfortunately, the limited solubility and low desorption ability of PZ have hindered its further application.[22] To address these issues, PZ-based amines, such as *N*-hydroxyethyl piperazine (HEP) and *N*-aminoethyl piperazine (AEP), have been developed for CO_2 capture. Replacing one secondary amine in HEP by a hydroxyethyl group increases solubility and regenerability, but simultaneously decreases the absorption capacity of CO_2.[27] In contrast, AEP shows improved absorption but a low desorption capacity for CO_2 due to the introduction of a primary amine group, which increases the binding affinity for CO_2.[28–30] A trade-off with respect to CO_2 capture by PZ-based absorbents clearly exists. Accordingly, the design and development of amine absorbents for CO_2 capture combining properties like absorption capacity, absorption/desorption rate, solubility, and stability remains a critical challenge.

Herein, we present a new kind of alcoholamines as chemical absorbents for efficient and cost-effective CO_2 capture. The obtained absorbents are constructed by simultaneously substituting the secondary amines of PZ with aminoethyl and hydroxyalkyl groups. The absorbents presented significantly improved solubility and thermal stability owing to the incorporated hydrophilic alkanol group and the existent naphthenic structure of PZ. More importantly, the obtained absorbents demonstrated enhanced CO_2 absorption/desorption performance, especially in terms of desorption rate and regenerability by virtue of the synergy of intramolecular amines. Experimental and computational studies revealed that the obtained amine absorbents have relatively lower absorption heat as well as regeneration energy consumptions compared to other conventional amines. Density functional theory (DFT) calculations are found to well correlate with the experimental results regarding CO_2 capture in various absorbents. Moreover, the reaction mechanism associated within CO_2 absorption/desorption in the absorbent was further elucidated via quantitative nuclear magnetic resonance (NMR) analysis. Overall, the newly developed alcoholamines will be the valuable and energy-efficient absorbents for CO_2 capture.

2 | MATERIALS AND METHODS

2.1 | Chemicals

Piperazine, *N*-aminoethylpiperazine, monoethanolamine, ethylene oxide, propylene oxide, 1,2-butene oxide, and methyl isobutyl ketone were purchased from commercial sources and used directly without further purification.

2.2 | Synthesis of PZ-derived alcoholamines

The PZ-derived alcoholamines, namely 1-(2-hydroxyethyl)-4-(2-aminoethyl)piperazine (HEAEP), 1-(2-hydroxypropyl)-4-(2-aminoethyl) piperazine (HPAEP), and 1-(2-hydroxybutyl)-4-(2-aminoethyl)piperazine (HBAEP), were prepared through a three-step process involving protection of the primary amino group, nucleophilic addition reaction with alkane oxide, and hydrolysis reaction (Scheme S1). Detailed information regarding synthesis, purification procedures, and characterization techniques are provided in the Supporting Information.

2.3 | Absorption/desorption experiments

An intermittent constant-pressure bubbling reactor, as shown in Figure 1, was used to investigate the absorption and desorption performance of the amine absorbents. The absorption process can be briefly described as follows. Initially, N_2 and CO_2 gases were introduced into a mixing tank, where they were combined into an N_2/CO_2 gas stream controlled by a mass flow meter. The gas stream entered the reactor containing the amine solution. The temperature of the reactor was maintained at a constant value with a water bath. The CO_2 absorbed by the solution was then passed through a condenser to a gas chromatograph to determine the vent concentration. Pure N_2 was used to extract the vapor during desorption. The temperature of the reactor was kept constant with an oil bath. Equilibrium solubility experiments for CO_2 absorption were conducted in a constant volume reactor, as depicted in Figure S1.[29] The quantity of CO_2 in the reactor was determined by analyzing the temperature and pressure variations before and after the injection of gas into the buffer tank. The quantity of CO_2 in the gas phase was determined from the equilibrium conditions of the reactor. The difference between these two quantities represents the extent to which CO_2 was absorbed by the amine solution. Vapor–liquid equilibrium (VLE) data corresponding to different CO_2 partial pressures are obtained by repeating experiments at different temperatures. The following semi-empirical model was adopted to correlate the obtained vapor–liquid phase equilibrium data.[31]

$$\ln P^{*}_{CO_2} = a + \frac{b}{T} + c \cdot \delta_p + \frac{d \cdot \delta_p}{T} + e \cdot {\delta_p}^2, \tag{1}$$

where δ_p is the loading amount of CO_2, mol·mol^{-1}; *a*, *b*, *c*, *d*, and *e* are the parameters.

Regeneration energy consumption (Q_{reg}, GJ·t^{-1} CO_2) was composed of three parts,[32–34] including reaction heat (Q_{reac}), sensible heat (Q_{sens}), and latent heat (Q_{latent}), and was expressed as $Q_{reg} = Q_{reac} + Q_{sens} + Q_{latent}$. Experimental and calculation details are presented in the Supporting Information.

2.4 | Computational methods

DFT calculations within a Gaussian 16 software package[35] were adopted to analyze the molecular surface electrostatic potential

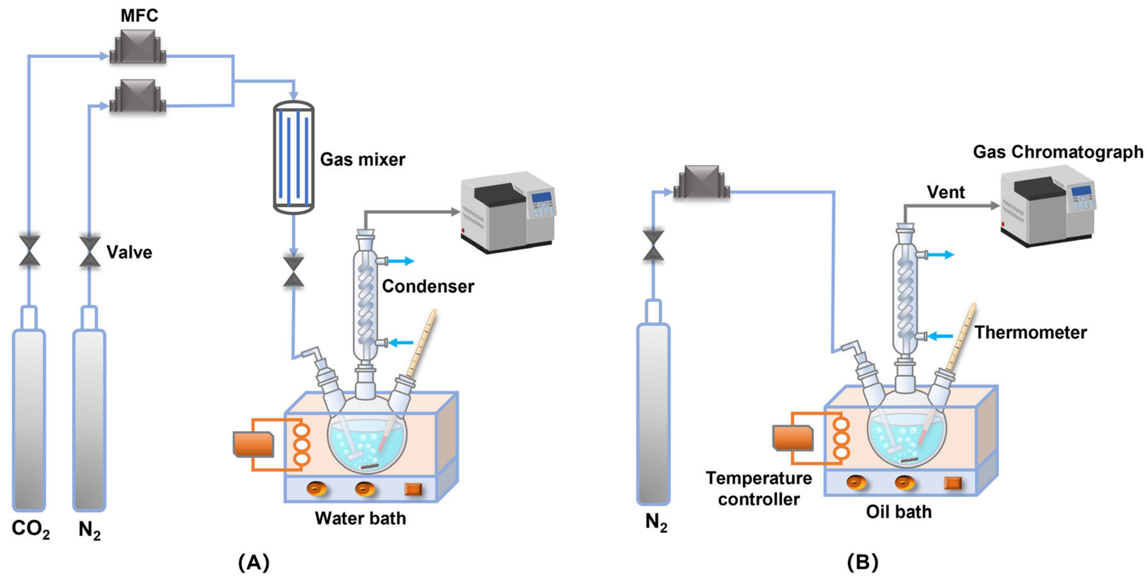

FIGURE 1 Schematic diagrams of (A) absorption and (B) desorption setups.

(ESP)[36] and the free energy barriers for CO_2 capture by amine groups.[37] Both molecular structure optimization and transition state (TS) searches were optimized at the B3LYP/6-31G* level of theory.[38–42] Because the B3LYP functional cannot describe the dispersion interactions, the keyword "Empirical Dispersion = GD3BJ"[43] was added. Solvent effects were determined using the universal solvation model (SMD).[44] The Multifunctional wavefunction analyzer (Multiwfn 3.8)[45,46] and Visual Molecular Dynamics (VMD 1.9.3)[47] were utilized to analyze and visualize the molecular ESP maps. Gibbs free energy of transition states, reactants, and products were calculated at the B3LYP/def2TZVPP level of theory.[37]

3 | RESULTS AND DISCUSSION

3.1 | Synthesis and characterization

The PZ-derived alcoholamines, namely 1-(2-hydroxyethyl)-4-(2-aminoethyl)piperazine (HEAEP), 1-(2-hydroxypropyl)-4-(2-aminoethyl) piperazine (HPAEP), and 1-(2-hydroxybutyl)-4-(2-aminoethyl)piperazine (HBAEP), were prepared through a three-step process that involved protecting the primary amino group, nucleophilic addition reactions with alkane oxide, and hydrolysis reaction (Scheme S1). In addition, the experimental conditions for the preparation of different absorbents were continuously optimized to produce high-purity samples (Figures S4–S15). For instance, the optimized reactant ratio of n_{AEP}:n_{MIBK}: n_{PO} = 1.0:4.0:1.7 for HPAEP resulted in a crude product with a 92% purity, which can be further refined to greater than 98% purity through additional purification steps (Figure S16). All three synthesized amines can be fully soluble in water, regardless of the ratio owing to their higher concentration of hydrophilic groups. NMR spectroscopy (Figures S17–S22) and mass spectrometry (Figures S23–S25) confirmed that the designed structures and the accurate molecular weight of different samples. Thermogravimetric (TG) and corresponding derivative thermogravimetric analysis revealed that HPAEP is more thermally stable than PZ (Figures S26, S27). The ESP of the molecular surface was adopted to explore molecular electrostatic interactions that provide predictive insight into specific reaction sites.[36] The Multiwfn[45,46] and VMD[46] visualized ESP diagrams for PZ, HEAEP, HPAEP, and HBAEP exhibited considerable negative electrostatic potentials surrounding their primary amines, along with more extensive negative ESP regions compared to PZ (Figure 2), which implies that the PZ-derived alcoholamines are likely to possess more active sites for CO_2 capture.

3.2 | CO_2 absorption/desorption performance

The CO_2 absorption/desorption performance of the absorbents was investigate at constant pressure using an intermittent bubbling reactor, which is a typical technique that has been widely employed to evaluate the absorption performance of amine absorbnets.[15,36,43,48] The CO_2 absorption/desorption performance of various samples with a 30 wt% concentration in solution was first evaluated at 40°C according to general industrial CO_2 absorption conditions.[49,50] Figure 3A illustrated that HPAEP exhibited a higher CO_2 loading amount (0.70 mol·mol^{-1}) compared to HEAEP (0.62 mol·mol^{-1}) and HBAEP (0.64 mol·mol^{-1}). However, the CO_2 loading amounts of the three synthesized amines were still lower than that of pristine PZ (0.72 mol·mol^{-1}). These differences are consistent with the lower pK_a values of the three synthesized amines compared to that of PZ (Table S1) since a higher pK_a value of the amine is beneficial for CO_2 absorption.[51] Unlike the reductions in CO_2 absorption loading capacity, insignificantly different initial absorption rates were observed during the first 10 min, which is ascribable to the continued presence of primary amines that rapidly form carbamate with CO_2, even after

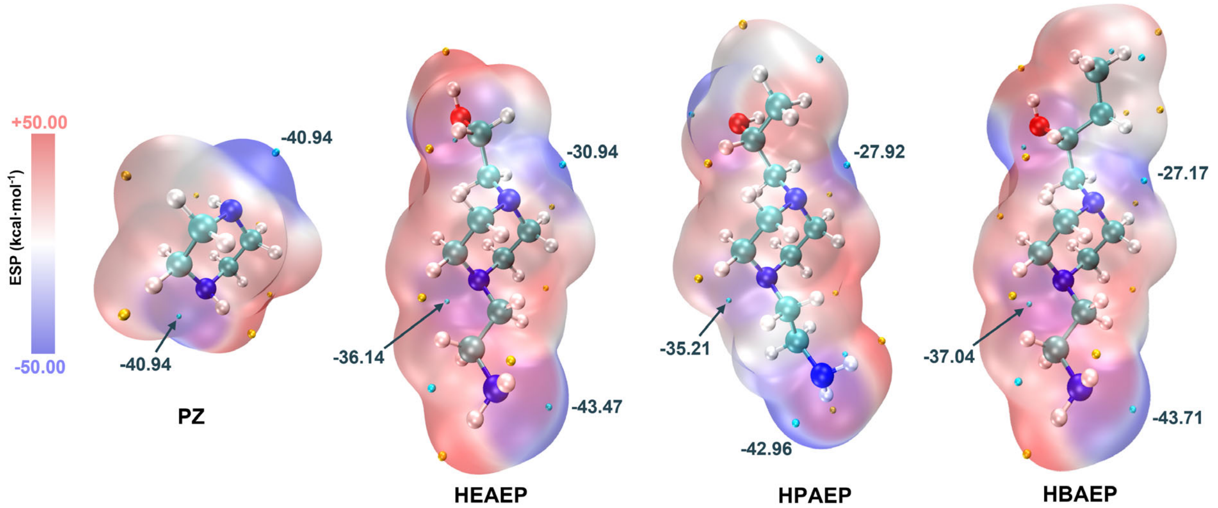

FIGURE 2 ESP diagrams of PZ, HEAEP, HPAEP, and HBAEP with the extreme points.

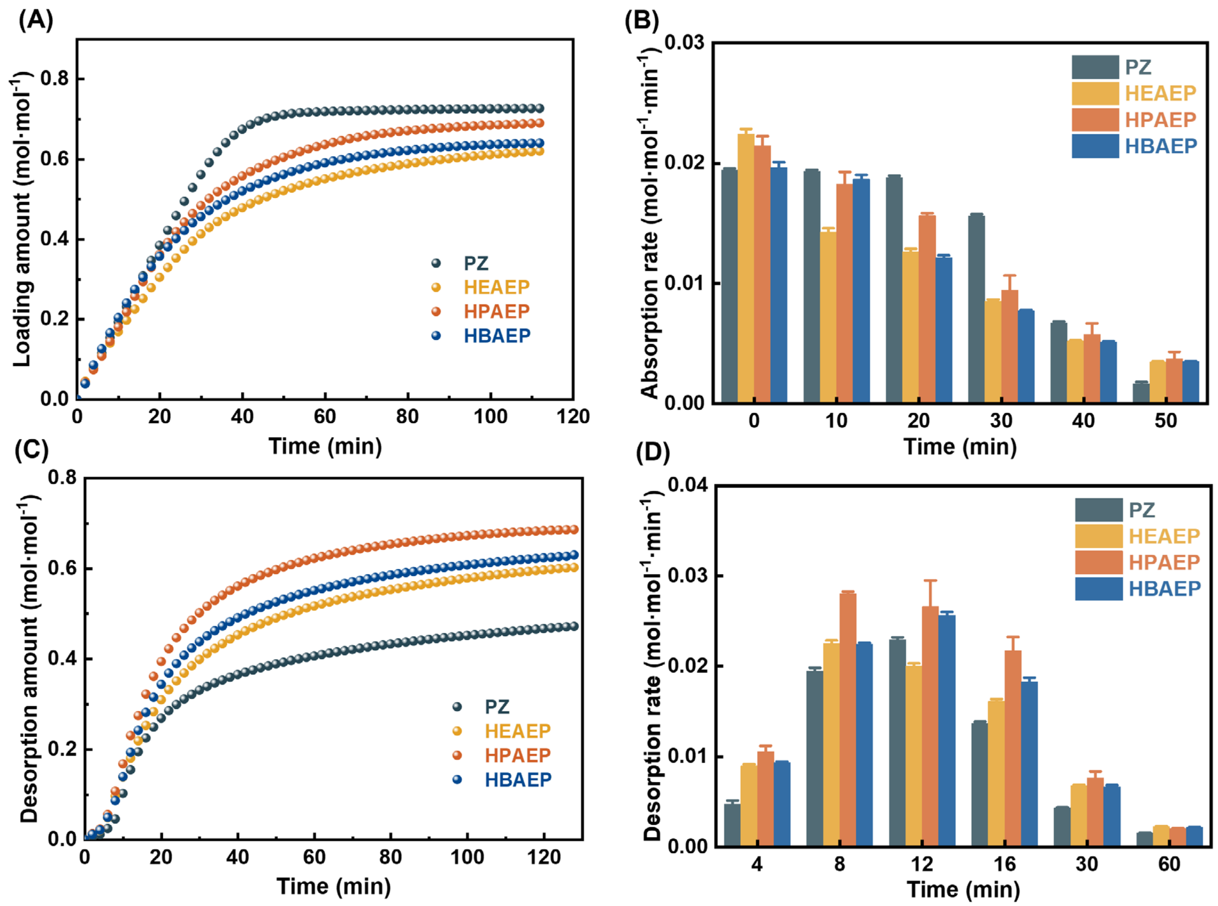

FIGURE 3 (A) Absorption loading amount, (B) absorption rate, (C) desorption amount and (D) desorption rate of different samples.

hydroxyalkyl modifications (Figure 3B). As displayed in Figure 3C, the desorption performances of the three prepared absorbents demonstrated a near-complete CO_2 desorption that surpassing the approximately 65% amount observed for PZ by over 1.5 times. Notably, it is evident that the desorption rate of each absorbent presented an upward trend during the first 10 minutes (Figure 3D) because the desired desorption temperature was not reached in the beginning (Figure S29). Moreover, the three synthesized absorbents demonstrated a higher desorption rate than PZ, which can be attributed to the potential regulation of alkalinity and steric hindrance effects by the intramolecular hydroxyalkyl and polyamine groups. HPAEP exhibited the highest desorption capacity and fastest desorption rate among the three synthesized absorbents because of the more positive ESP surrounding its primary amine group (Figure 2), which is beneficial for reducing the affinity between primary amino groups and CO_2,[36] thereby promoting desorption performance by decreasing the stability of the carbamate.

In practical absorption processes, an ideal absorbent should be highly stable and reusable for long-term use in industrial separation.[17] The absorbent is frequently not fully desorbed due to the equipment and cost of the regeneration process, leading to its recycling in the form of a lean amine solution. The residual CO_2 in the lean amine solution significantly affects the absorption capacity, absorption rate, and absorption efficiency during the subsequent absorption process. To further understand the regenerability of the absorbent, the second CO_2 absorption performance of the desorbed lean amine solution was then investigated. In marked contrast to the first absorption results (Figure S30), the second CO_2 absorption capacity and initial CO_2 absorption rate of the three synthesized amines were found to be significantly greater than those of PZ. Considering the superior performance of HPAEP in both CO_2 absorption and desorption processes, as well as its structural similarity to other synthesized amines, HPAEP was selected for further in-depth investigations. Figure 4A illustrates the recyclability of HPAEP across five cycles of absorption and desorption, along with viscosity, and highlights its stability and efficiency throughout the entire cycle process. In addition, the ^{13}C NMR spectra acquired before and after five cycles indicate no significant alteration in amine structure (Figure S31), confirming the chemical stability of HPAEP during CO_2 capture process. Moreover, the simultaneous thermal analysis of HPAEP indicates that the primary weight loss range of HPAEP was between 280 and 300°C, with no noticeable weight loss occurring below 200°C (Figure S26). Altogether, the excellent stability and reusability results suggest that HPAEP is a promising absorbent for CO_2 capture.

Further investigations were carried out to explore the CO_2 absorption/desorption behavior of HPAEP at different concentrations. The results (Figures 4B and S32–S34) illustrated that the CO_2 loading capacity, absorption rate, desorption amount, and desorption rate all decreased with increasing HPAEP concentration, which is rationalized by increases in solution viscosity that resulted in lower mass transfer and lower amine capture efficiency as a consequence (Figure S35).[52] However, when the concentration of HPAEP surpasses 40 wt%, the increased viscosity leads to a more significant reduction in CO_2 absorption efficiency. Therefore, similar to other amine absorbents,[50] it is recommended that HPAEP be operated at an optimal concentration in the range of 30–40 wt%. Furthermore, water molecules may affect the ions balance in a solution via two possible reactions, as demonstrated by the equations

$$\mathrm{HPAEP} + \mathrm{H_2O} \rightarrow \mathrm{HPAEPH^+} + \mathrm{OH^-}, \tag{2}$$

and

$$\mathrm{HPAEPCOO^-} + \mathrm{H_2O} \rightarrow \mathrm{HPAEP} + \mathrm{HCO_3}^-. \tag{3}$$

Equation (2) suggests that water molecules accelerate HPAEP hydrolysis by generating a greater number of OH^- that continuously react with CO_2, while Equation (3) produces higher quantities of HCO_3^- and HPAEP that simultaneously promote both absorption and desorption processes.

3.3 | Evaluation of the regeneration energy consumption

The energy consumption during the regeneration process is the predominant limitation of amine-scrubbing-based CO_2 capture technology.[53] Regeneration energy consumption typically comprises three main parts,[33,54,55] namely the latent heat (Q_{latent}) associated with solvent vaporization, the sensible heat (Q_{sens}) required to heat the absorbent, and the reaction heat (Q_{reac}) associated with the release of CO_2. Differentiating these three parts is crucial for an in-depth investigation

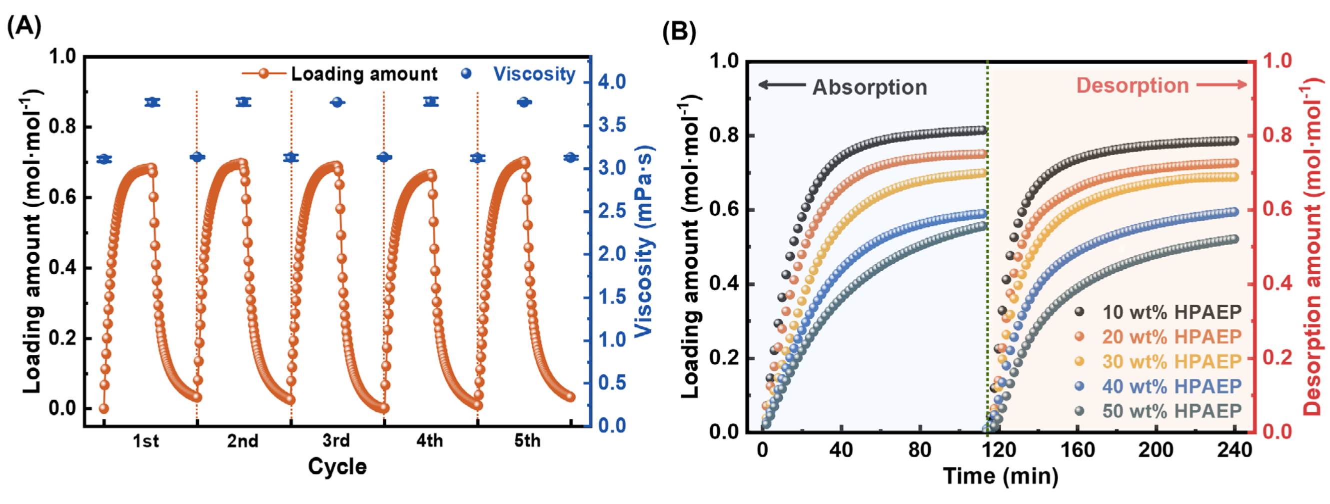

FIGURE 4 (A) CO_2 absorption/desorption cycle of HPAEP and (B) CO_2 absorption/desorption amount of HPAEP at different concentrations.

of the regeneration process of the absorbents. Consequently, the Q_{reg} of HPAEP was analyzed to further explore its energy-saving benefits. Q_{reac} was determined by plotting the VLE curves of different samples at various temperatures. As shown in Figures 5A and S2, the VLE curve for MEA obtained in the present work is well accordance with that previously reported by Lee et al.,[56] which highlights the reliability of the experimental setup adopted in this study. In addition, three replicate experiments on HPAEP were performed to ensure the reliability of the VLE curves (Figure S36). Figure 5A reveals that HPAEP exhibits a CO_2 equilibrium partial pressure that increases steadily with increasing CO_2 loading and absorption temperature. Notably, slope of the VLE curve of HPAEP is smoother than that of MEA, consistent with enhanced sensitivity of its CO_2 loading to alterations in partial pressure. Such characteristic provides a significant advantage for amine regeneration under swing pressure conditions. VLE curves were also acquired for PZ for comparative analysis purposes (Figure S37). Empirical equations and the Gibbs-Helmholtz equation were adopted to estimate ΔH_{abs} value for both HPAEP and PZ.[29,54,57] Typically, MEA exhibits a higher ΔH_{abs} value with a value of over 80 kJ·mol^{-1},[58] while the ΔH_{abs} value of PZ is around 70–90 kJ·mol^{-1} (Figure 5B). The higher ΔH_{abs} value of MEA and PZ are attributable to stronger absorption heats between their strongly alkaline amine groups and CO_2 molecules.[31] In contrast, HPAEP has a significantly lower ΔH_{abs} of approximately 30–50 kJ·mol^{-1} compared to MEA and PZ owing to the modestly lower alkalinities of its amine groups, a consequence of the incorporated hydroxyl and polyamine groups (Figure 5B).

Typically, the specific heat capacity and the evaporation of the solvent are applied to determine Q_{sens} and Q_{latent} (Figures S38 and S39).[25,29] For comparison, the Q_{reg} of MEA (Figure S40) and PZ (Figure S41) were estimated and their lowest values of Q_{reg} are plotted in Figure 5C. The Q_{reg} of HPAEP was evaluated at different levels of regeneration efficiency. The results clearly demonstrate that the Q_{reac} of HPAEP increases with increasing regeneration efficiency, which can be attributed to the progressive increase in pH during the desorption process that does not benefit CO_2 release. However, the Q_{latent} of HPAEP was observed to gradually increase with increasing regeneration efficiency, whereas its Q_{sens} initially decreases and then increases. In addition, Q_{sens} is associated with the desorption amount and the desorption rate of CO_2.[29,59] Figure 5D depicts that a relatively large amount of CO_2 is released during the early stages of CO_2

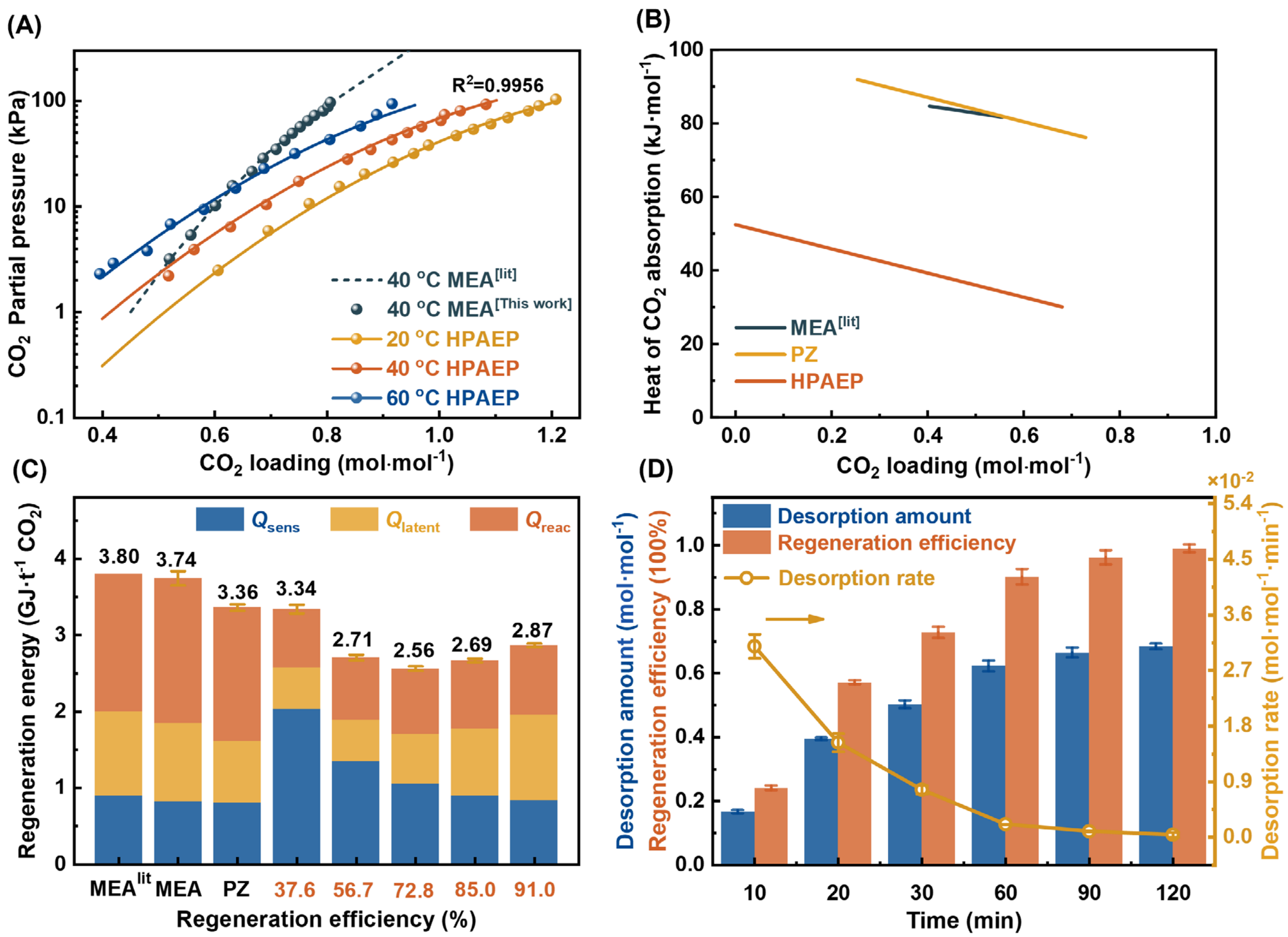

FIGURE 5 (A) VLE curves of MEA and HPAEP (reported curve, dash line; experimental curve, dot line; fitted curve, solid line). (B) Heat of CO_2 absorption as a function of CO_2 loading for MEA, PZ, and HPAEP. (C) Regeneration energy consumption of HPAEP under different regeneration efficiency, MEA and PZ are included for comparison. (D) Desorption performance and regeneration efficiency of HPAEP as a function of time.

desorption, leading to a rapid decrease in Q_{sens}, after which it tends to stabilize as the CO_2 desorption rate gradually decreases. Q_{latent} is related to the evaporation of water and the desorption rate of CO_2. The desorption rate of CO_2 is the primary factor that affects Q_{latent} during the initial stage of desorption. Q_{latent} increases significantly with decreasing CO_2 desorption rate because of the evaporation of water. Apparently, Q_{reac}, Q_{latent}, and Q_{sens} simultaneously influence the overall Q_{reg} of HPAEP. As the regeneration efficiency increases, the Q_{reg} initially decreases and subsequently increases. A minimum Q_{reg} of 2.56 $GJ \cdot t^{-1}$ CO_2 was recorded at an efficiency of 78.6%, which is only 67% of that required when using MEA as an absorbent for CO_2 capture.[54]

3.4 | DFT calculations

Theoretically, the Gibbs free energy barrier reflects the reaction rate of the elementary reaction to a certain extent.[60,61] Figure 6 presents the free energy barrier for the initial state (IS), TS, and final state (FS) associated with PZ, HEAEP, HPAEP, and HBAEP according to the zwitterion reaction mechanism that involves the primary/secondary amine groups and CO_2.[49] HPAEP was calculated to have a considerably lower free energy barrier between IS and TS, which suggests that it is more likely to react with CO_2. This observation in consistent with the more negative of the surface ESP of HPAEP compared to that of PZ (Figure 2). A highly negative ESP renders a molecule more nucleophilic or capable of generating electrons, which favors the binding of amine group with CO_2.[36] Additionally, it also plays a key role in the higher initial absorption rate of HPAEP compared to that of PZ (Figure 3B). However, the lower pH associated with the lower pK_a HPAEP hampers maintaining high absorption rates in the long term compared to PZ.[19] Significantly, HPAEP exhibits a substantial lower free energy barrier from the FS to TS compared to PZ, indicating a potentially rapid release of CO_2. Similar to HPAEP, the free energy barriers of HEAEP and HBAEP from the IS to the TS are apparently lower than that of PZ, which is consistent with their faster initial CO_2 absorption rates (Figure 3B). Specifically, HEAEP presented the lowest free energy barrier during the transition from IS to TS, while HBAEP exhibited the highest free energy barrier. The hydroxyalkyl side chains increase steric hindrance, which significantly affect the free energy barrier. Specifically, longer alkyl side chains result in higher free energy barriers.[48] Moreover, it is noteworthy that HPAEP possesses the lowest free energy barrier when transitioning from FS to TS, consistent with its exceptional desorption performance

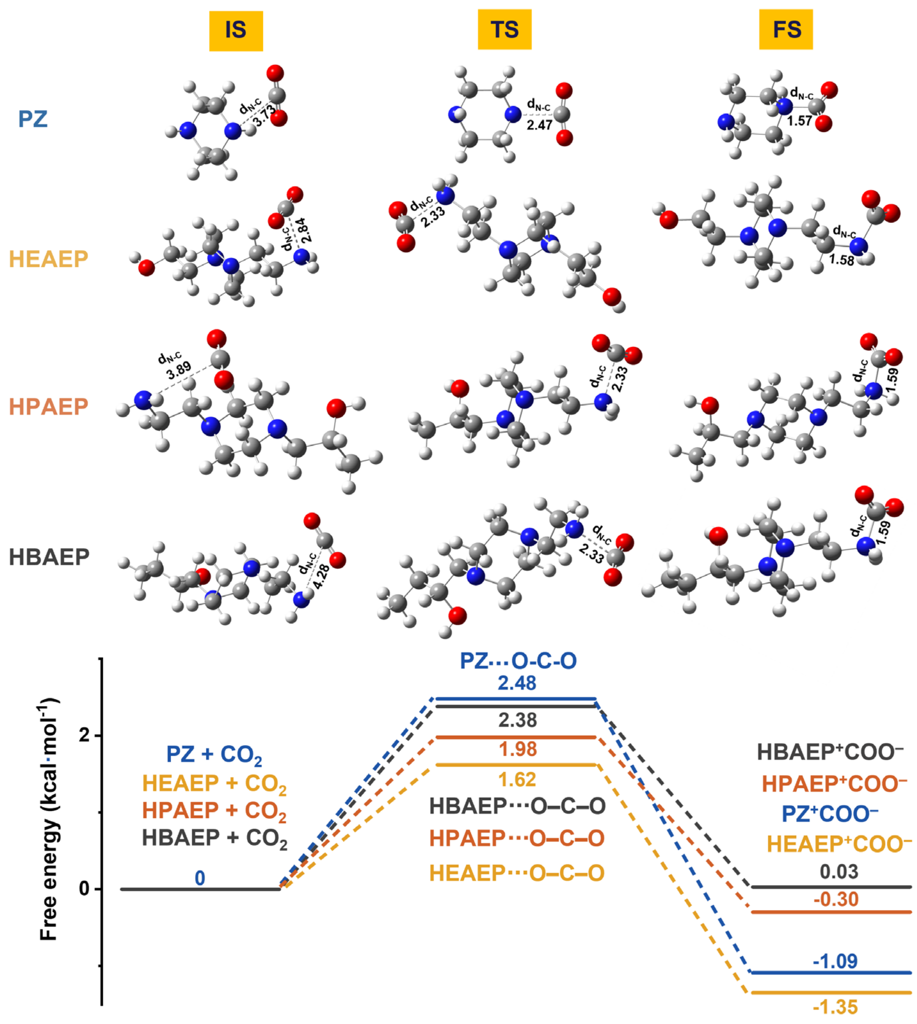

FIGURE 6 Free energy barrier diagrams of PZ, HEAEP, HPAEP, and HBAEP. The calculated temperature and pressure are 298 K and 1 bar.

(Figure 3C, D) and more positive ESP (Figure 2) compared with those of HEAEP and HBAEP. A more positive ESP allows for more efficient release of CO_2.[36]

3.5 | Reaction mechanism of CO_2 capture

^{13}C NMR was utilized to investigate the reaction mechanism and the distribution of substances involved in the capture of CO_2 by HPAEP during absorption and desorption processes. Differentiating HCO_3^-/CO_3^{2-} and HPAEP/$HPAEPH^+$ pairs by NMR spectra is challenging because of the rapid proton transfer reactions.[62] The ion contents at various CO_2 loading levels were recorded and analyzed as depicted in Figure 7A, B. During the absorption process, CO_2 initially exists primarily in the form of carbamate in solution. The concentration of $HPAEPCOO^-$ was observed to decrease as the CO_2 loading level surpassed 0.44 mol·mol^{-1}, while the CO_3^{2-}/HCO_3^- content progressively increased. This observation is attributed to a reduction in solution pH, which promotes the hydrolysis of $HPAEPCOO^-$ and results in the formation of HPAEP and HCO_3^-. To elucidate the influence of the modified tertiary amine group on CO_2 capture performance, a comparison between the CO_2 absorption process of PZ (Figure 7C, D) and that of HPAEP was performed. Similar to HPAEP, the CO_2 in the PZ solution exists

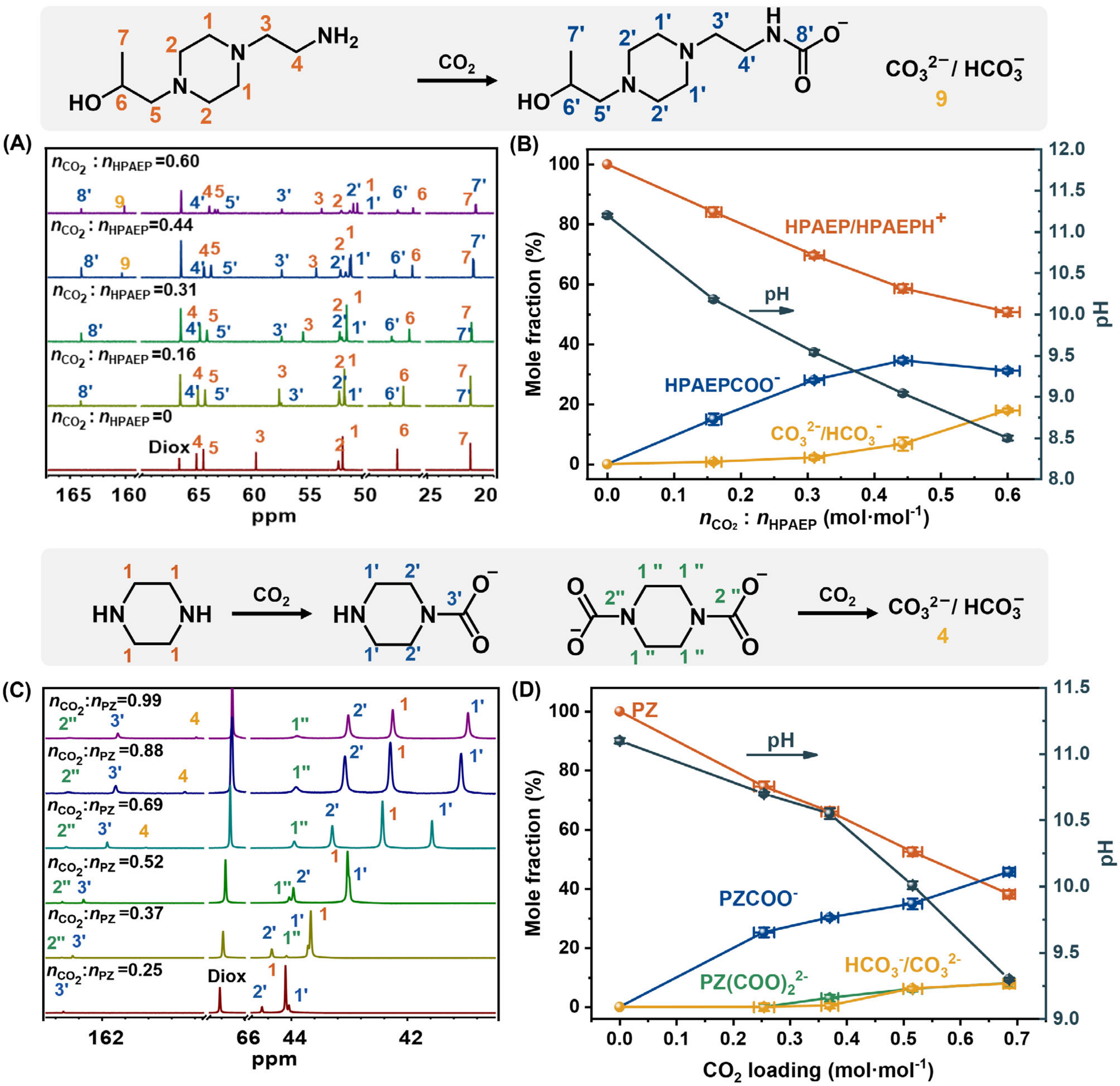

FIGURE 7 ^{13}C NMR spectra of the absorption process in (A) HPAEP and (C) PZ solutions by adding of CO_2. The concentration profiles of the different ions during the CO_2 absorption process in (B) HPAEP and (D) PZ solutions.

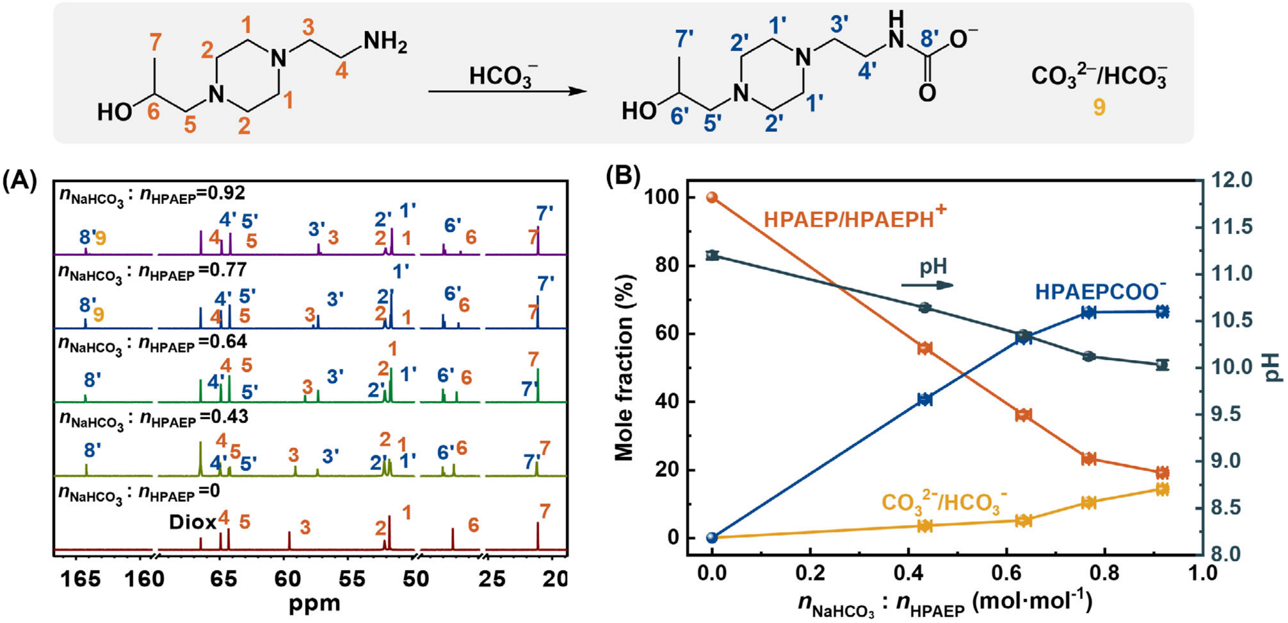

FIGURE 8 (A) ^{13}C NMR spectra and (B) corresponding concentration profiles of the different ions during the CO_2 absorption process in HPAEP solution by adding of $NaHCO_3$.

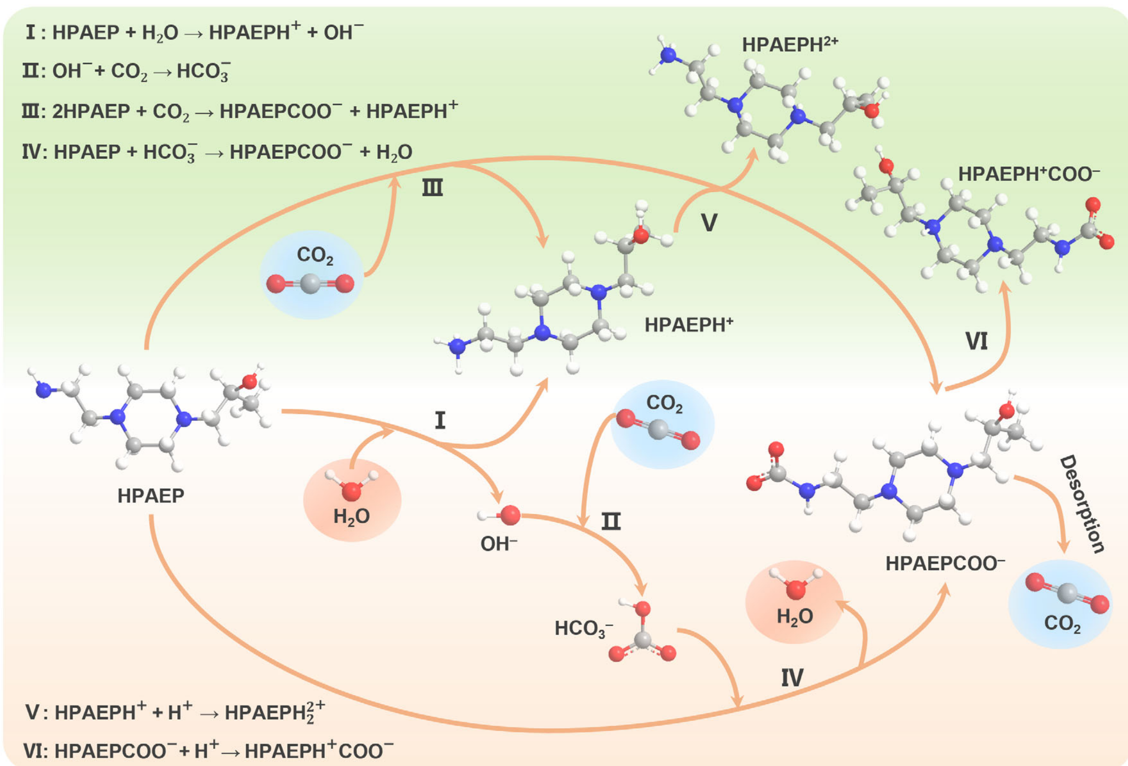

FIGURE 9 Schematic illustration of the CO_2 capture mechanism for the HPAEP solution.

primarily in the form of carbamate during the initial absorption stage. However, CO_3^{2-}/HCO_3^- becomes observable as the CO_2 loading surpassing 0.4 mol·mol^{-1}, while the concentration of carbamate gradually stabilizes. Remarkably, CO_3^{2-}/HCO_3^- is evidently detachable at higher concentrations in the HPAEP solution, which significantly influences the desorption performance and the energy consumption required for regeneration.[19,20,63] Notably, the substances in the HPAEP solution were found to exhibit the reverse distribution trend during the desorption process compared to that observed during the absorption process (Figure S42).

To explore the conversions of HPAEP and HCO_3^- by substituting $NaHCO_3$ for CO_2 in order to analyze variations in the ion content in solution. As depicted in Figure 8, it is evidenced that carbamate is formed in solution, which confirms that CO_2 can react with primary amine in the form of H_2CO_3/HCO_3^- to produce carbamate in aqueous solution. HCO_3^-/CO_3^{2-} appears in solution with increasing $NaHCO_3$ concentration, which stabilizes the carbamate content as a consequence. It is worth noting that carbonation reaction involving $NaHCO_3$ results in a higher pH and carbamate content than that involving CO_2 at the same level, which suggests that the reaction between HCO_3^- and HPAEP (Equation (3)) depends on the pH of the solution. A higher pH promotes the formation of carbamate, while a lower pH favors the generation of HCO_3^-. Additionally, the experiment further confirmed that water affects the equilibrium states of absorption and desorption (Equations (2) and (3)), which is consistent with the CO_2 absorption/desorption performance of HPAEP at different concentrations (Figure 4B).

Based on the above analysis and discussion, the proposed reaction mechanism for CO_2 capture by HPAEP can be illustrated in Figure 9. A portion of HPAEP undergoes hydrolysis to release OH^- and $HPAEPH^+$ in aqueous solution (Reaction I), resulting in an alkaline solution with a pH value ranging from 11 to 12. Subsequently, the released OH^- subsequently reacts with CO_2 to generate HCO_3^- (Reaction II), with the remaining HPAEP in solution reacting with CO_2/HCO_3^- to produce $HPAEPCOO^-$ (Reactions III and IV). The reversibility of all reactions involved in CO_2 capture by HPAEP depend on the pH and temperature of the solution. Especially, the desorption process almost inverse to the absorption process at elevated temperatures. It is noteworthy that proton exchange reaction potentially occurs between the tertiary and primary amino groups (Reactions V and VI). Also, the intramolecular synergy between the primary and tertiary amines contributes significantly to reinforcing both the absorption and desorption processes.

4 | CONCLUSIONS

In summary, we developed a new kind of PZ-derived alcoholamines for CO_2 capture through the synergy of their intramolecular amines. The newly obtained alcoholamines exhibited significant improvements in solubility and thermal stability, as well as greatly enhanced CO_2 capture efficiency and reusability compared to pristine PZ. The DFT calculated surface ESP and free energy barrier results correlate well with that the improvements of CO_2 absorption/desorption by the obtained alcoholamines. In addition, we demonstrated that the optimal absorbent of HPAEP shows exceptional cycle stability, with a regeneration energy consumption as low as 2.56 $GJ \cdot t^{-1}$ CO_2. Moreover, ^{13}C NMR analysis of the reaction between HPAEP and CO_2/HCO_3^- provided insight into the absorption/desorption and the pH-driven carbamate conversion mechanism. Overall, the PZ-derived alcoholamines developed in this study have promising potential for application in emerging separation technologies, such as phase change separation, high-temperature flash evaporation, and vacuum stripping. Also, the present study offers valuable insights into the design and development of novel absorbents toward the efficient and cost-effective CO_2 capture demands.

AUTHOR CONTRIBUTIONS

Shaojun Jia: Data curation (equal); formal analysis (equal); investigation (equal); methodology (equal); writing – original draft (equal). **Yao Jiang:** Conceptualization (equal); funding acquisition (equal); project administration (equal); resources (equal); supervision (equal); writing – original draft (equal); writing – review and editing (lead). **Songtao Zheng:** Data curation (equal); formal analysis (equal); investigation (equal). **Yi Li:** Data curation (equal); investigation (equal). **Yan Wu:** Data curation (equal); formal analysis (equal). **Xiao-Qin Liu:** Resources (equal); software (lead). **Peng Cui:** Conceptualization (equal); funding acquisition (equal); project administration (equal); resources (equal); supervision (equal).

ACKNOWLEDGMENTS

This work was supported by the Major Science and Technology Project of Anhui Province (201903a07020004), the National Natural Science Foundation of China (22208078), the Graduate Academic Innovation Project of Anhui Province (2022xscx019), the Fundamental Research Funds for the Central Universities (JZ2023HGTB0226), and the State Key Laboratory of Materials-Oriented Chemical Engineering (SKL-MCE-22B11).

DATA AVAILABILITY STATEMENT

The numerical data from Figures 2–8 are tabulated in the Supporting Information. The data that support this study are available from the corresponding author upon reasonable request.

ORCID

Shaojun Jia https://orcid.org/0009-0003-4097-9719
Yao Jiang https://orcid.org/0000-0002-2316-8274

REFERENCES

1. Liu HL, Jiang XT, Idem R, Dong SL, Tontiwachwuthikul P. AI models for correlation of physical properties in system of 1DMA2P-CO_2-H_2O. *AIChE J*. 2022;68(9):e17761.
2. Matthews HD, Wynes S. Current global efforts are insufficient to limit warming to 1.5°C. *Science*. 2022;376(6600):1404-1409.
3. Meinshausen M, Lewis J, McGlade C, et al. Realization of paris agreement pledges may limit warming just below 2°C. *Nature*. 2022;604(7905):304-309.
4. Bui M, Adjiman CS, Bardow A, et al. Carbon capture and storage (CCS): the way forward. *Energ Environ Sci*. 2018;11(5):1062-1176.
5. Li K, Leigh W, Feron P, Yu H, Tade M. Systematic study of aqueous monoethanolamine (MEA)-based CO_2 capture process: techno-economic assessment of the MEA process and its improvements. *Appl Energy*. 2016;165:648-659.
6. Adams Ii TA, Barton PI. High-efficiency power production from coal with carbon capture. *AIChE J*. 2010;56(12):3120-3136.
7. Sullivan M, Rodosta T, Mahajan K, Damiani D. An overview of the Department of Energy's CarbonSAFE initiative: moving CCUS toward commercialization. *AIChE J*. 2020;66(4):e16855.

8. He T, Liu ZX, Son H, Gundersen T, Lin WS. Comparative analysis of cryogenic distillation and chemical absorption for carbon capture in integrated natural gas liquefaction processes. *J Clean Prod*. 2023;383: 135264.
9. Zeng SJ, Zhang X, Bai LP, et al. Ionic-liquid-based CO_2 capture systems: structure, interaction and process. *Chem Rev*. 2017;117(14): 9625-9673.
10. Lin JB, Nguyen TTT, Vaidhyanathan R, et al. A scalable metal-organic framework as a durable physisorbent for carbon dioxide capture. *Science*. 2021;374(6574):1464-1469.
11. Yang X, Rees RJ, Conway W, Puxty G, Yang Q, Winkler DA. Computational modeling and simulation of CO_2 capture by aqueous amines. *Chem Rev*. 2017;117(14):9524-9593.
12. Theo WL, Lim JS, Hashim H, Mustaffa AA, Ho WS. Review of pre-combustion capture and ionic liquid in carbon capture and storage. *Appl Energy*. 2016;183:1633-1663.
13. Zheng W, Luo Q, Liu S, et al. New method of kinetic modeling for CO_2 absorption into blended amine systems: a case of MEA/EAE/3-DEA1P trisolvent blends. *AIChE J*. 2022;68(6):e17628.
14. Rochelle GT. Amine scrubbing for CO_2 capture. *Science*. 2009; 325(5948):1652-1654.
15. Cao L, Dong H, Zhang X, et al. Highly efficient carbon dioxide capture by a novel amine solvent containing multiple amino groups. *J Chem Technol Biotechnol*. 2015;90(10):1918-1926.
16. Morgan JC, Bhattacharyya D, Tong C, Miller DC. Uncertainty quantification of property models: methodology and its application to CO2-loaded aqueous MEA solutions. *AIChE J*. 2015;61(6):1822-1839.
17. Liu H, Li M, Luo X, Liang Z, Idem R, Tontiwachwuthikul P. Investigation mechanism of DEA as an activator on aqueous MEA solution for postcombustion CO_2 capture. *AIChE J*. 2018;64(7):2515-2525.
18. Hu XY, Huang JT, He XW, et al. Analyzing the potential benefits of trio-amine systems for enhancing the CO_2 desorption processes. *Fuel*. 2022;316:123216.
19. Xiao M, Cui D, Yang Q, et al. Advanced designer amines for CO_2 capture: interrogating speciation and physical properties. *Int J Greenhouse Gas Control*. 2019;82:8-18.
20. Zhang R, Luo X, Yang Q, Cao F, Chen S, Liang Z. Impact of the inter- and intramolecular tertiary amino group on the primary amino group in the CO_2 absorption process. *Ind Eng Chem Res*. 2016;55(26):7210-7217.
21. Zhang R, Yang Q, Yu B, Yu H, Liang Z. Toward to efficient CO_2 capture solvent design by analyzing the effect of substituent type connected to N-atom. *Energy*. 2018;144:1064-1072.
22. Freeman SA, Davis J, Rochelle GT. Degradation of aqueous piperazine in carbon dioxide capture. *Int J Greenhouse Gas Control*. 2010;4(5): 756-761.
23. Freeman SA, Rochelle GT. Thermal degradation of aqueous piperazine for CO_2 capture. 1. Effect of process conditions and comparison of thermal stability of CO_2 capture amines. *Ind Eng Chem Res*. 2012; 51(22):7719-7725.
24. Delgado S, Valentin B, Bontemps D, Authier O. Degradation of amine solvents in a CO_2 capture plant at lab-scale: experiments and modeling. *Ind Eng Chem Res*. 2018;57(18):6057-6067.
25. Rochelle G, Chen E, Freeman S, van Wagener D, Xu Q, Voice A. Aqueous piperazine as the new standard for CO_2 capture technology. *Chem Eng J*. 2011;171(3):725-733.
26. Zhao YM, Zhang YC, Liu Q, et al. Energy-efficient carbon dioxide capture using piperazine (PZ) activated EMEA plus DEEA water lean solvent: performance and mechanism. *Sep Purif Technol*. 2023;316: 123761.
27. Li H, Le Moullec Y, Lu J, Chen J, Marcos JCV, Chen G. Solubility and energy analysis for CO_2 absorption in piperazine derivatives and their mixtures. *Int J Greenhouse Gas Control*. 2014;31:25-32.
28. Balchandani SC, Mandal B, Dharaskar S. Stimulation of CO_2 solubility in reversible ionic liquids activated by novel 1-(2-aminoethyl piperazine) and bis (3-aminopropyl) amine. *Sep Purif Technol*. 2021; 262:118260.
29. Shen L, Liu F, Shen Y, et al. Novel biphasic solvent of AEP/1--propanol/H_2O for CO_2 capture with efficient regeneration performance and low energy consumption. *Sep Purif Technol*. 2021;270: 118700.
30. Yang CN, Li TC, Tantikhajorngosol P, Sema T, Xiao M, Tontiwachwuthikul P. Evaluation of novel aqueous piperazine-based physical-chemical solutions as biphasic solvents for CO_2 capture: initial absorption rate, equilibrium solubility, phase separation and desorption rate. *Chem Eng Sci*. 2023;277:118852.
31. Chen X, Rochelle GT. Aqueous piperazine derivatives for CO_2 capture: accurate screening by a wetted wall column. *Chem Eng Res Des*. 2011;89(9):1693-1710.
32. Zhao B, Liu FZ, Cui Z, et al. Enhancing the energetic efficiency of MDEA/PZ-based CO_2 capture technology for a 650 MW power plant: process improvement. *Appl Energy*. 2017;185:362-375.
33. Nwaoha C, Idem R, Supap T, et al. Heat duty, heat of absorption, sensible heat and heat of vaporization of 2-Amino-2-Methyl-1-propanol (AMP), Piperazine (PZ) and Monoethanolamine (MEA) tri-solvent blend for carbon dioxide (CO_2) capture. *Chem Eng Sci*. 2017;170: 26-35.
34. Liu F, Fang MX, Dong WF, et al. Carbon dioxide absorption in aqueous alkanolamine blends for biphasic solvents screening and evaluation. *Appl Energy*. 2019;233:468-477.
35. Gaussian 16 Rev. C.01 [computer program]. 2016.
36. Gao G, Jiang W, Li X, et al. Novel assessment of highly efficient polyamines for post-combustion CO_2 capture: absorption heat, reaction rate, CO_2 cyclic capacity, and phase change behavior. *Sep Purif Technol*. 2023;306:122615.
37. Wei D, Luo QL, Ouyang T, et al. An experimental and theoretical study on the effects of amine chain length on CO_2 absorption performance. *AIChE J*. 2023;69(4):e17960.
38. Ditchfield R, Hehre WJ, Pople JA. Self-consistent molecular-orbital methods. IX. An extended Gaussian-type basis for molecular-orbital-studies of organic molecules. *J Chem Phys*. 1971;54(2):724-728.
39. Feller D. The role of databases in support of computational chemistry calculations. *J Comput Chem*. 1996;17(13):1571-1586.
40. Pritchard BP, Altarawy D, Didier B, Gibson TD, Windus TL. New basis set exchange: an open, up-to-date resource for the molecular sciences community. *J Chem Inf Model*. 2019;59(11):4814-4820.
41. Schuchardt KL, Didier BT, Elsethagen T, et al. Basis set exchange: a community database for computational sciences. *J Chem Inf Model*. 2007;47(3):1045-1052.
42. Stephens PJ, Devlin FJ, Chabalowski CF, Frisch MJ. Ab initio calculation of vibrational absorption and circular dichroism spectra using density functional force fields. *J Phys Chem*. 1994;98(45):11623-11627.
43. Grimme S, Antony J, Ehrlich S, Krieg H. A consistent and accurate ab initio parametrization of density functional dispersion correction (DFT-D) for the 94 elements H-Pu. *J Chem Phys*. 2010;132(15): 154104.
44. Cossi M, Rega N, Scalmani G, Barone V. Energies, structures, and electronic properties of molecules in solution with the C-PCM solvation model. *J Comput Chem*. 2003;24(6):669-681.
45. Lu T, Chen FW. Multiwfn: a multifunctional wavefunction analyzer. *J Comput Chem*. 2012;33(5):580-592.
46. Zhang J, Lu T. Efficient evaluation of electrostatic potential with computerized optimized code. *Phys Chem Chem Phys*. 2021;23(36): 20323-20328.
47. Humphrey W, Dalke A, Schulten K. VMD: visual molecular dynamics. *J Mol Graph*. 1996;14(1):33-38.
48. Xiao M, Liu HL, Idem R, Tontiwachwuthikul P, Liang ZW. A study of structure-activity relationships of commercial tertiary amines for post-combustion CO_2 capture. *Appl Energy*. 2016;184:219-229.

49. El Hadri N, Quang DV, Goetheer EL, Zahra MRA. Aqueous amine solution characterization for post-combustion CO_2 capture process. *Appl Energy*. 2017;185:1433-1449.
50. Gur TM. Carbon dioxide emissions, capture, storage and utilization: review of materials, processes and technologies. *Prog Energy Combust Sci*. 2022;89:100965.
51. Chowdhury FA, Yamada H, Higashii T, Goto K, Onoda M. CO_2 capture by tertiary amine absorbents: a performance comparison study. *Ind Eng Chem Res*. 2013;52(24):8323-8331.
52. Ma MM, Liu YC, Chen YL, et al. Regulatory mechanism of a novel non-aqueous absorbent for CO_2 capture using 2-amino-2-methyl-1-propanol: low viscosity and energy efficient. *J CO_2 Util*. 2023;67:102277.
53. Lv B, Sun C, Liu N, Li W, Li S. Mass transfer and kinetics of CO_2 absorption into aqueous monoethanolamine/1-hydroxyethy-3-methyl imidazolium glycinate solution. *Chem Eng J*. 2015;280:695-702.
54. Kim H, Hwang SJ, Lee KS. Novel shortcut estimation method for regeneration energy of amine solvents in an absorption-based carbon capture process. *Environ Sci Technol*. 2015;49(3):1478-1485.
55. Zhang S, Ye X, Lu Y. Development of a potassium carbonate-based absorption process with crystallization-enabled high-pressure stripping for CO_2 capture: vapor–liquid equilibrium behavior and CO_2 stripping performance of carbonate/bicarbonate aqueous systems. *Energy Procedia*. 2014;63:665-675.
56. Lee JI, Otto FD, Mather AE. Equilibrium between carbon dioxide and aqueous monoethanolamine solutions. *J Appl Chem Biotechnol*. 2010;26(1):541-549.
57. Zhang S, Shen Y, Shao P, Chen J, Wang L. Kinetics, thermodynamics, and mechanism of a novel biphasic solvent for CO_2 capture from flue gas. *Environ Sci Technol*. 2018;52(6):3660-3668.
58. Kim YE, Yun SH, Choi JH, et al. Comparison of the CO_2 absorption characteristics of aqueous solutions of diamines: absorption capacity, specific heat capacity, and heat of absorption. *Energy Fuel*. 2015;29(4):2582-2590.
59. Zhou XW, Shen Y, Liu F, et al. A novel dual-stage phase separation process for CO_2 absorption into a biphasic solvent with low energy penalty. *Environ Sci Technol*. 2021;55(22):15313-15322.
60. Xie HB, He N, Song ZQ, Chen JW, Li XH. Theoretical investigation on the different reaction mechanisms of aqueous 2-amino-2-methyl-1-propanol and monoethanolamine with CO_2. *Ind Eng Chem Res*. 2014;53(8):3363-3372.
61. Luo QL, Dong R, Yoon B, et al. An experimental/computational study of steric hindrance effects on CO_2 absorption in (non)aqueous amine solutions. *AIChE J*. 2022;68(7):e17701.
62. Zhang XW, Zhang R, Liu HL, Gao HX, Liang ZW. Evaluating CO_2 desorption performance in CO_2-loaded aqueous tri-solvent blend amines with and without solid acid catalysts. *Appl Energy*. 2018;218:417-429.
63. Zhang R, Liang ZW, Liu HL, et al. Study of formation of bicarbonate ions in CO_2-loaded aqueous single 1DMA2P and MDEA tertiary amines and blended MEA-1DMA2P and MEA-MDEA amines for low heat of regeneration. *Ind Eng Chem Res*. 2016;55(12):3710-3717.

SUPPORTING INFORMATION

Additional supporting information can be found online in the Supporting Information section at the end of this article.

How to cite this article: Jia S, Jiang Y, Zheng S, et al. Highly efficient capture of CO_2 through the synergy of intramolecular amines within piperazine-derived alcoholamines. *AIChE J*. 2024;70(6):e18439. doi:10.1002/aic.18439